Torchia, D. A., & Piez, K. A. (1973) *J. Mol. Biol. 76*, 419–424.
Urry, D. W. (1976) *Faraday Discuss. Chem. Soc. 61*, 205–216.
Urry, D. W., Okamoto, K., Harris, R. D., Hendrix, C. F., & Long, M. M. (1976) *Biochemistry 15*, 4083–4089.
Urry, D. W., Trapane, T. L., Sugano, H., & Prasad, K. U. (1981) *J. Am. Chem. Soc. 103*, 2080–2089.
Urry, D. W., Trapane, T. L., Long, M. M., & Prasad, K. V. (1983) *J. Chem. Soc., Faraday Trans. 1 79*, 853–868.
Volpin, D., Pasquali-Ronchetti, I., Urry, D. W., & Gotte, L. (1976) *J. Biol. Chem. 251*, 6871–6873.
Yoon, K., Davidson, J. M., Boyd, C. May, M., LuValle, P., Ornstein-Goldstein, N., Smith, J., Indik, Z., Ross, A., Golub, E., & Rosenbloom, J. (1985) *Arch. Biochem. Biophys. 241*, 684–691.

Articles

Crystal Structure of Cytochrome *c* Peroxidase Compound I[†]

Steven L. Edwards,[*,‡] Nguyen huu Xuong,[‡,§,∥] Ronald C. Hamlin,[§] and Joseph Kraut[‡]
Departments of Chemistry, Physics, and Biology, University of California, San Diego, La Jolla, California 92093
Received July 17, 1986; Revised Manuscript Received October 24, 1986

ABSTRACT: We have compared the 2.5-Å crystal structure of yeast cytochrome *c* peroxidase (CCP) with that of its semistable two-equivalent oxidized intermediate, compound I, by difference Fourier and least-squares refinement methods. Both structures were observed at −15 °C. The difference Fourier map reveals that formation of compound I causes only small positional adjustments of a few tenths of an angstrom. The map's most pronounced feature is a pair of positive and negative peaks bracketing the heme iron position. Least-squares refinement shows that the iron atom moves about 0.2 Å toward the distal side of the heme. No significant difference density is evident near the side chains of Trp-51 or Met-172, each of which has been proposed to be the site of the electron paramagnetic resonance (EPR) active radical in compound I. However, the second most prominent feature of difference density is a negative peak near the side chain of Thr-180, which, according to the results of least-squares refinement, moves by 0.15 Å in the direction of Met-230. These observations, together with the results of mutagenesis experiments [Fishel, L. A., Villafranca, J. E., Mauro, J. M., & Kraut, J. (1987) *Biochemistry 26*, 351–360; Goodin, D. B., Mauk, A. G., & Smith, M. (1986) *Proc. Natl. Acad. Sci. U.S.A. 83*, 1295–1299] in which Trp-51 and Met-172 have been replaced without loss of the EPR radical signal in compound I, lead us to consider the possibility that the radical site lies within a cluster composed of the side chains of Met-230, Met-231, and Trp-191. This cluster is contiguous with Thr-180 and about 10 Å from the heme plane on the proximal side.

Compound I (also termed compound ES) is a semistable enzyme intermediate that results from the oxidation of cytochrome *c* peroxidase (ferrocytochrome *c*:H_2O_2 oxidoreductase, EC 1.11.1.5; CCP)[1] by its substrate, peroxide (Abrams et al., 1942). Various peroxides, including H_2O_2, react with CCP to remove two reducing equivalents from the enzyme to form compound I, which is then rereduced in two successive one-electron steps by ferrocytochrome *c*. The reaction scheme may be written (Yonetani & Ray, 1966)

$$\text{CCP} + \text{ROOH} \rightarrow \text{compound I} + \text{ROH}$$

$$\text{compound I} + \text{cyt-}c(\text{Fe}^{2+}) + \text{H}^+ \rightarrow \text{compound II} + \text{cyt-}c(\text{Fe}^{3+})$$

$$\text{compound II} + \text{cyt-}c(\text{Fe}^{2+}) + \text{H}^+ \rightarrow \text{CCP} + \text{cyt-}c(\text{Fe}^{3+}) + \text{H}_2\text{O}$$

where ROOH is an alkyl peroxide or hydrogen peroxide. Compound I is not an enzyme–substrate complex in the usual Michaelis–Menten sense, but rather, it is an intermediate species in which the first step of the enzyme-catalyzed reaction, reductive cleavage of the peroxide bond, has already occurred.

The importance of CCP as an object of study derives in part from certain functional similarities to respiratory cytochrome oxidase. The latter is a heme-containing multisubunit complex that catalyzes the reduction of molecular oxygen to water by ferrocytochrome *c* as the ultimate step in the electron-transport chain. CCP similarly contains heme as a prosthetic group, catalyzes the reduction of an oxygen–oxygen bond by ferrocytochrome *c*, and has been shown to substitute as a terminal oxidase in yeast when the respiratory oxidase is inhibited (Erecinska et al., 1973). Thus, as a simpler model for the more complicated and experimentally elusive cytochrome oxidase, CCP has become the focus of much study and speculation.

The initial crystal structure of CCP was reported by our laboratory in 1980 (Poulos et al., 1980), and the 1.7-Å refinement in 1984 (Finzel et al., 1984). A structure-based mechanism suggested by Poulos and Kraut (1980a,b) incor-

[†] This work was supported by National Science Foundation Grant DMB-8511656 awarded to J.K. Ng.h.X. acknowledges support from National Institutes of Health Grant RR 01644 for the UCSD Data Collection Resource for Protein Crystallography in addition to a special grant from the NSF Biological Instrument Program (PCM-8400547) and a grant for low-temperature experimentation (DMB-8510860).
[‡] Department of Chemistry.
[§] Department of Physics.
[∥] Department of Biology.

[1] Abbreviations: CCP, cytochrome *c* peroxidase; ENDOR, electron nuclear double resonance; EPR, electron paramagnetic resonance; EXAFS, extended X-ray absorption fine structure; HRP, horseradish peroxidase.

0006-2960/87/0426-1503$01.50/0

porated most of the kinetic and physical data reported up to 1980. It is generally accepted that the two oxidizing equivalents of CCP compound I are divided between a heme-centered oxyferryl ion, Fe^{IV}=O (Lang et al., 1976; Chance et al., 1986b), and a radical located at some as yet unidentified amino acid side chain or group of side chains. In contrast, the analogous horseradish peroxidase compound I probably carries its second oxidizing equivalent in the form of a porphyrin cation radical (Dolphin et al., 1971).

The identity of the radical site in CCP compound I has continued to be the subject of vigorous controversy. Early UV absorption and EPR measurements (Yonetani & Ray, 1965; Yonetani et al., 1966b) were interpreted as implying that one of the oxidizing equivalents of compound I exists as a free radical on an aromatic amino acid side chain. A second set of experiments by Coulson and Yonetani (1972) examined the decay products of compound I by amino acid analysis and showed that tryptophans and tyrosines were being destroyed. At this point in the chronology, the crystal structure of ground-state CCP revealed that the indole ring of Trp-51 is located less than 5 Å from the ligand binding site, parallel to and in van der Waals contact with the distal face of the heme (Poulos et al., 1980). Trp-51 was therefore assumed to be the radical site in the mechanism proposed by Poulos and Kraut (1980a).

At about the same time, conflicting spectroscopic evidence was presented by Hoffman et al. (1979). Their interpretation of electron nuclear double resonance (ENDOR) experiments with CCP compound I led these investigators to rule out a tryptophan as the site of the radical. They proposed instead that the radical is more likely to resemble a two-sulfur dimeric radical cation [$(R_2SSR_2)^+$] model (Musker & Wolford, 1976). Although a Met-Met sequence does indeed occur at position 230–231 in CCP, when the crystal structure became available, it appeared that these side chains are too far from the peroxide binding site (over 10 Å) and have too great a separation (6 Å) between sulfur atoms. As an alternative, Hoffman et al. (1981) therefore focused on Met-172 (formerly numbered 171), which is situated 5.6 Å from the heme on the proximal side. Since no second sulfur atom is nearby to participate in their proposed dimeric radical cation, however, they suggested that a Met-172 radical could instead be stabilized by interaction with the heme or with some neighboring side chain.

Meanwhile, in another line of investigation, we have attempted to elucidate the dynamics of the active site of CCP by soaking heme ligands into crystals of the parent enzyme and examining the consequent structural perturbations by the difference Fourier technique. Ligands we have studied so far include HCN (Poulos et al., 1978), HF (Edwards et al., 1984), and NO (Edwards, 1981). These experiments showed small but easily observable movements in response to ligand binding. Among other things, they have demonstrated that the side chain of Arg-48, on the distal side of the heme, can make a conformational adjustment to optimize its interaction with ligands.

Encouraged by these results, in particular by the extreme sensitivity of the difference Fourier method when applied to a well-refined structure like CCP, it occurred to us that a similar examination of compound I might point to the locus of the radical. We hoped that the electronic redistribution accompanying the formation of a radical, especially a positively charged radical, would cause small but detectable positional shifts of nearby atoms with some partial negative charge character. Indeed, such an experiment had been suggested as long ago as 1966 (Yonetani et al., 1966), although the required techniques were not available until recently. Even though collecting a complete set of diffraction data for a stable protein crystal has now become fairly routine, doing the same for a short-lived enzyme intermediate has only recently become feasible with the development of high-speed area detector diffractometers and compatible low-temperature technology (Xuong et al., 1978).

Experimental Procedures

Cytochrome *c* peroxidase was purified from bakers' yeast by the method of Nelson et al. (1977). Parent CCP crystals were grown by the Jansonius method of seeding with visible microcrystals (Thaller et al., 1981). Once this method was perfected, we found it possible to grow crystals with similar morphology that could be fully converted to compound I without cracking. This reproducibility was important in obtaining high-quality X-ray data and in achieving good scaling between data sets. The average crystal used was approximately $0.7 \times 0.3 \times 0.3$ mm. Although larger crystals were available, they did not convert to compound I as completely and also tended to crack in the conversion process. The compound I crystals' space group is $P2_12_12_1$ with unit cell dimensions of $107.79 \times 76.90 \times 51.61$ Å, identical with the dimensions of the parent crystals.

Parent crystals were converted to compound I by soaking them for 20 min in a synthetic mother liquor containing 50 mM potassium phosphate, pH 6.0, and 35% (v/v) 2-methyl-2,4-pentanediol plus 10 mM H_2O_2, following which excess H_2O_2 was removed by transferring the crystals into a peroxide-free synthetic mother liquor. Each crystal was then mounted in a glass capillary and positioned with its *c* axis along the capillary axis. These operations were carried out in a cold room at 2 °C. Initially, we attempted to cool the compound I crystals sufficiently to make them indefinitely stable. Although methylpentanediol is a good cryosolvent, the crystals would not tolerate concentrations higher than 35% (v/v) without cracking. At this methylpentanediol concentration the crystals could be cooled down to −15 °C but not below, without loss of crystal order due to freezing. By trial and error, we determined that at 35% methylpentanediol and −15 °C we could only collect X-ray data for about 4 h before the compound I content of the crystals suffered significant decay. The compound I content of the crystals was determined at the end of each data set by dissolving the crystals in 0.1 M potassium phosphate buffer and comparing the visible spectrum absorbance at 560 nm, a peak characteristic of compound I, to that at 515 nm, an isosbestic point (Erman & Yonetani, 1975).

We have been using the locally developed multiwire area detector (Xuong et al., 1978) to collect most of the CCP-related diffraction data. This apparatus employs software that allows the data to be substantially processed on-line (Howard et al., 1985). A drawback, however, is that the crystal must be precisely aligned before data collection is begun, a procedure that sacrifices at least 1 h of X-ray exposure. Because loss of this initial hour of compound I lifetime would considerably compromise the quality of the resulting data, we decided to attempt data collection from crystals that were only approximately aligned by saving raw detector images on magnetic tape. Then, after data collection is terminated owing to decay of compound I, the final precise alignment is carried out by use of the stored detector images. Details of the procedure are described next.

Converted crystals were transferred to the Mark II multiwire area detector diffractometer equipped with a low-temperature device set at −15 °C. Each crystal was quickly attached to the goniostat, and 5 min of exposure were expended

to bring the crystal within about 2 deg of alignment by viewing electronic images. Data collection was then started on a selected region of reciprocal space. A data set consists of a series of electronic detector images collected while the crystal is rotated around the ω axis by 0.1 deg per image. The exposure time per image was adjusted (usually 45 s) so that a full ω sweep took about 4 h. At the end of a data set, 20 min of further X-ray exposure was required to determine the alignment angles within 0.1 deg. At this point the crystal was removed from the goniostat and returned to the cold room for analysis. Reflection intensities were later extracted from the stored raw detector images by running the standard automatic alignment programs on the stored images to determine the exact orientation matrix. Once the matrix values were known, the standard data collection program could be used to process the stored images.

The resulting intensity measurements from six crystals, corrected for Lorentz, polarization, and background, were merged. A total of 53 700 observations of 14 600 unique reflections were merged with a scaling residual of symmetry-related reflections,[2] R_{sym} = 5.1%. The merged set constitutes a complete sphere of data to 2.5-Å resolution with an average of 3.7 observations of each unique reflection; 97% of the measurements were above 2σ. Subsequent Fourier calculations included all terms to 2.5 Å and were carried out with the XTAL system of computer programs (Hall et al., 1980). The average compound I content of the crystals was judged to be approximately 80% at the end of data collection as determined by visible spectrum measurements made on the dissolved crystals. No attempt was made to measure the EPR spectrum of the crystals.

In order to enhance the quality of the ultimate difference Fourier, we attempted to collect new parent data under the same conditions as for the compound I data. Parent crystals were grown by the procedure described above. Those selected for the data collection were on the average twice the volume of those used for the compound I data. Unfortunately, the last batch of crystals grown for parent data collection tended to freeze at −15 °C so we elected to raise the temperature slightly, to −12 °C, for two of the six data crystals, affecting about 40% of the data. A total of 264 500 observations of 39 700 unique reflections were measured from six different crystals. These data represent all of the reflections to 2.0-Å resolution and about half of the remaining reflections to 1.8 Å. The data scaled together with an agreement R_{sym} = 4.9% with over 95% of the measurements greater than 2σ.

Least-Squares Refinement. To provide a valid starting model for the compound I refinement, the parent structure was refined against new diffraction data collected on parent crystals at essentially the same low temperature, −15 °C (see above). The starting model for the low-temperature refinement was the refined room temperature structure (Finzel et al., 1984). We applied the conjugate-gradient least-squares procedure of Hendrickson and Konnert (1980) as described by Finzel et al. with the following exception: all target σ values for bond lengths, bond angles, and torsion angles were reduced by half to enforce better geometry on the resulting model.

Refinement was initiated against the low-resolution data up to 2.3 Å and converged after four cycles with a residual of R = 0.17. At this point, 76 water molecules with temperature factors larger than 40 Å^2 were removed from the model. The resolution limit of the data was increased to 2.1 Å, and four more cycles of refinement were run, converging at an R = 0.166. In order to unbias the water positions from those of the original model, all 188 waters were removed from the model and two more cycles of refinement run to generate phases that were used to calculate an $F_o - F_c$ and a $2F_o - F_c$ map. Each of the 188 water positions was checked against the maps to assess its peak height and the potential for hydrogen bonding to the rest of the model; 171 of these were accepted as valid water positions. Refinement was continued in groups of three cycles with the amount of data being gradually increased. Between each group of cycles, difference Fouriers were calculated to search for additional water molecules and side chains that required manual adjustment. The final cycles of refinement including all of the data produced a residual of R = 0.17. A total of 282 water molecules were ultimately accepted.

The major differences between the −15 °C parent structure and the room temperature parent structure were a lower average temperature factor (B = 17 Å^2 compared to B = 22 Å^2) and a movement of the side chain of Arg-48, which appeared to be positioned about 1.5 Å closer to the ligand binding site at the lower temperature.

Least-squares refinement of the compound I structure was initiated using the refined parent structure just described as the starting model. The refinement converged after three cycles with an average positional shift of 0.11 Å. For these cycles, the iron atom had been restrained in the plane of the pyrrole nitrogens. To determine the iron position more accurately, the iron atom was removed from the model and three more cycles of refinement were performed, in order to produce phases that were less biased by the restrained iron position. The resulting phases were used to calculate a difference Fourier map, $F_o - F_c$, which showed a peak near the heme normal located about 0.1 Å on the distal side of the plane of the pyrrole nitrogens. This was judged to indicate the position of the iron. Further cycles of refinement with the restraints removed from the iron caused it to move to the position of the peak observed in the difference Fourier. This position is about 0.2 Å from the iron position in the parent structure, toward the distal side of the heme. After all solvent molecules with high temperature factors (>50 Å^2) were removed, the resulting residual was R = 0.19. Our attempt to refine the ferryl oxygen position led to an unreasonable location for the ligand, probably due to the short bond distance to the electron-dense iron atom and the lack of sufficiently high resolution to separate their peaks. However, a final $F_o - F_c$ difference map, with calculated structure factors including the iron atom, showed a peak near the heme normal, approximately 1.9 Å from the iron position. Evidently this peak represents the ferryl oxygen ligand, which was omitted from the model. Because at 2.5-Å resolution the peak is probably distorted by the adjacent iron density, the 1.9-Å distance would likely be an overestimate of the Fe=O bond distance. We believe that the correct bond distance is closer to 1.7 Å, consistent with the bond distances found by EXAFS on CCP compound I (Chance et al., 1986b) and HRP compound I (Chance et al., 1984).

Results and Discussion

The Difference Map. The −15 °C compound I *minus* parent difference Fourier map is shown in Figure 1. It is contoured at $\pm 3.5\sigma$ and $\pm 5\sigma$, where σ is the root mean square difference density over an entire unit cell. The difference map is superimposed on a backbone representation of the CCP molecule.

[2] The scaling residual of symmetry-related reflections is calculated from

$$R_{sym} = \sum_{hkl} \frac{\sum_i |I_i - \langle I \rangle|}{\sum_i I_i}$$

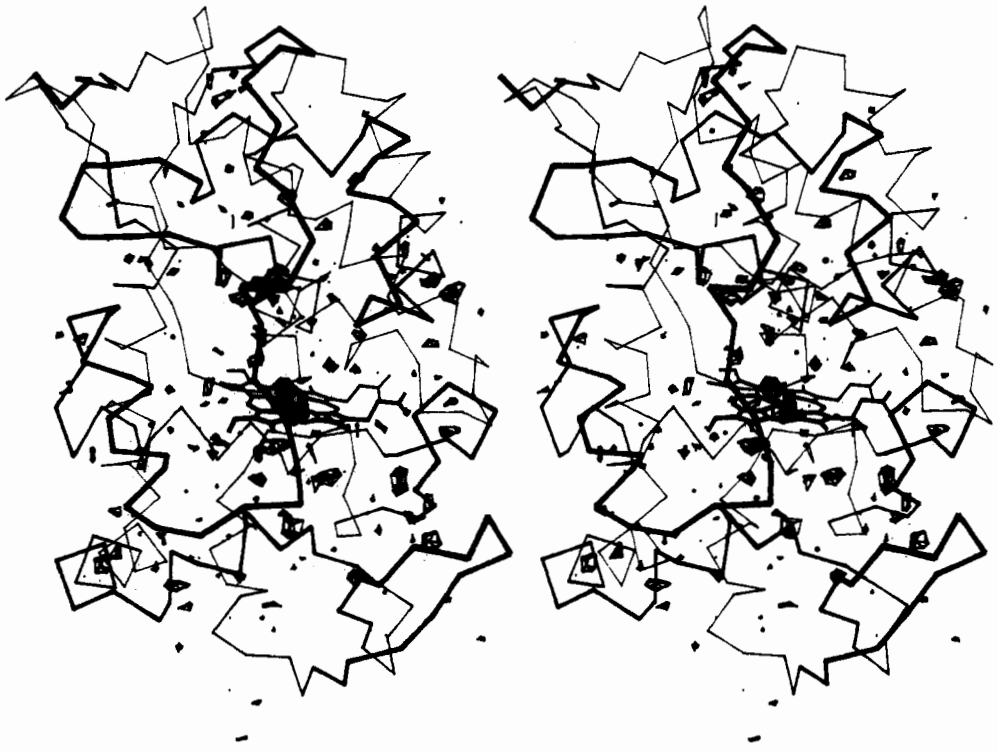

FIGURE 1: Compound I minus parent cytochrome *c* peroxidase difference Fourier map superimposed on a backbone model of the parent structure. Contour levels are at $\pm 3.5\sigma$ and $\pm 5.0\sigma$.

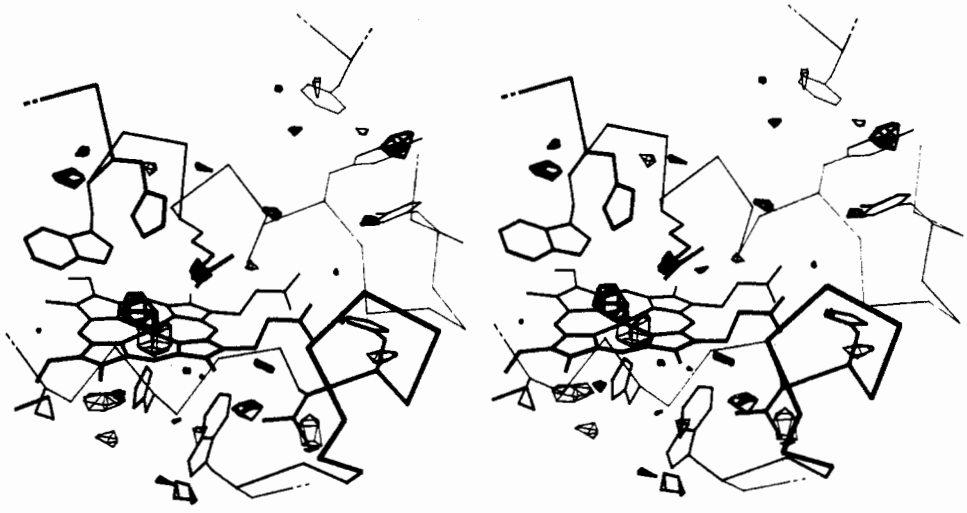

FIGURE 2: A more detailed view of the compound I minus parent CCP difference Fourier map around the heme region contoured at $\pm 4\sigma$. The positive density is contoured with thick lines and the negative density with thin lines. Broken lines indicate discontinuities in the backbone.

Inspection of the map shows that only subtle structural perturbations occur on formation of compound I, chiefly in the vicinity of the heme group. None of the peaks are large enough to represent the addition of a new atom as a result of oxidation. A closer view of the heme region, including some side chains, is shown in Figure 2. The largest perturbation is represented by a pair of positive and negative peaks at the 6σ level, bracketing the heme iron atom and indicating its movement toward the distal side of the heme plane. The magnitude of this displacement, 0.2 Å, was estimated by least-squares refinement, as described later.

The second largest feature in the difference map centers on a 5σ hole near the side chain of Thr-180. The immediate neighbors of Thr-180, namely, Trp-191 and His-181 (see Figure 2), are also touched by somewhat less prominent difference density. Near the surface of the molecule in the vicinity of the heme propionates a positive peak (about 4.5σ) appears at Tyr-42. In addition, two peaks of positive difference density occur along the side chain of Arg-48. Although the difference map, upon initial inspection, is rather complicated looking, most of its features became interpretable after least-squares refinement of the compound I structure and comparison with the refined, low-temperature parent CCP structure. This comparison revealed that, on formation of compound I, small (less than 0.3 Å) but coordinated perturbations occur around the heme that are consistent with its oxidation state. The possible functional significance of these observations is discussed below.

A particularly noteworthy feature of the compound I difference map is the absence of difference density near certain residues. As already mentioned, one of the goals of this study was to locate the radical in compound I. We hoped that difference density associated with some amino acid side chain would help to identify the radical site. Two candidates for

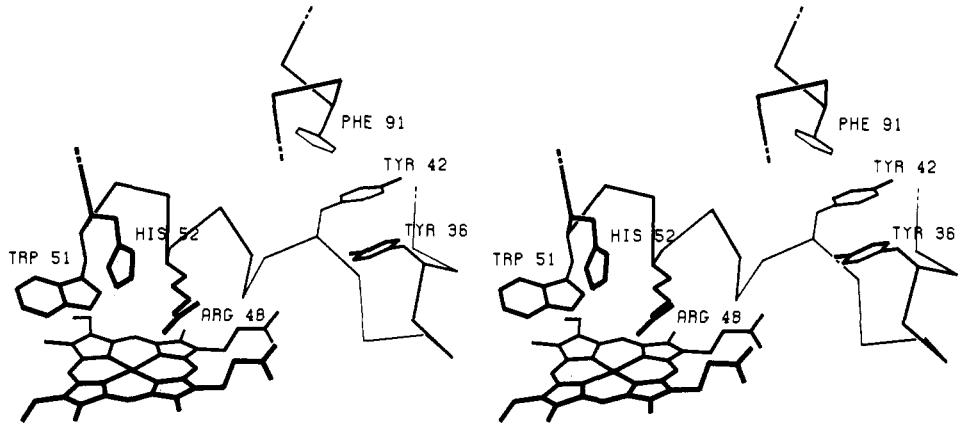

FIGURE 3: Identification of selected residues on the distal side of the heme. The tyrosines are near the surface of the molecule.

this site have been the indole ring of Trp-51 (Poulos & Kraut, 1980a) and the sulfur of Met-172 (Hoffman et al., 1981). However, examination of the regions around these side chains reveals no significant difference density. While this observation does not in itself rule out either residue as the site of the free radical, it agrees with the negative results of mutagenesis experiments (see below). However, finding strong difference density close to the side chain of Thr-180 does point to another possible location for the radical, as discussed below.

It is appropriate to interject a cautionary note here concerning interpretation of the difference Fourier map. In other experiments we have found that small changes in solvent composition perturb side-chain conformations on the surface of the molecule. In particular, that part of the surface including Tyr-42 is especially sensitive (see Figure 2 for density and Figure 3 for label), probably because it borders the largest solvent channel in the crystal. Most likely this solvent perturbation effect accounts for certain features observed near Tyr-42 in the compound I *minus* parent difference map. We are more confident about the other features already described because they are in the interior of the molecule and are confirmed by the least-squares refinement.

Least-Squares Refinement. Comparison of the refined compound I structure with the refined parent structure reveals many small adjustments, none more than 0.5 Å. The most significant of these are as follows.

The iron atom is displaced by 0.2 Å from the proximal side toward the distant side of the heme. This displacement causes the imidazole ring of proximal His-175 to move in concert by the same amount, presumably in order to maintain its bond with the heme iron. The refined imidazole N^{ϵ} to iron distance is 2.0 Å, in adequate agreement with the bond distance of 1.91 Å found by Chance et al. (1986b) by EXAFS measurements. In addition, the entire heme group slides 0.1 Å further into the heme crevice.

Certain oxygen atoms are slightly displaced toward the sulfurs of Met-230 and Met-231. The side chain of Thr-180 moves about 0.2 Å toward Met-230. Examination of the Met-230, Met-231 vicinity also reveals that three backbone carbonyl oxygen atoms (residues 188, 189, and 190) tilt toward Met-230, while the only nearby water molecule (water-495, 6.2 Å from the sulfur atom of Met-231) moves 0.2 Å directly toward the sulfur of Met-231.

The positional adjustments described so far pertain to the side chains and backbone carbonyls of a loop made up of residues 175–190. This loop, which has the geometry of an antiparallel β-pair, carries the side chains of His-181, Asn-184, and Ser-185, which hydrogen bond to the propionate of heme pyrrole IV (Finzel et al., 1984) as does the backbone NH of His-181. The entire loop appears to undergo a complicated twist as a result of the combined motions of the heme group, of His-175, and of Thr-180. The twist may be functionally important because it involves residues at the proposed binding site for cytochrome *c* (Poulos & Kraut, 1980b).

On the distal side of the heme, the side chain of Arg-48 moves about 0.3 Å toward the ligand binding site. The adjustment may be due to a stronger hydrogen bond to the ferryl oxygen atom, but it probably also reflects the movement of the entire heme group.

Since the movements just described are rather small, it is important to mention some additional evidence that supports our belief in their reality. First, we point out that certain other side-chain motions evidently maintain hydrogen bonding even though hydrogen-bond distances are not enforced by restraints included in the refinement program. In particular, as the side chain of His-175 moves to maintain a coordination bond with the iron atom, we observe that the side chain of Asp-235 also moves toward His-175 to maintain a hydrogen bond between the two side chains. As a second example, we focus on the movement of water-495. Comparison of the two parent structures (−15 °C and room temperature) shows that this water molecule occupies the same position in both parent structures, moves 0.2 Å toward Met-231 in compound I, and then in the decay product (D. H. Anderson et al., personal communication) returns to essentially the same position as in the parent structures.

Thus, all the displacements we describe above, although quite small, are at least consistent with chemical logic and other experimental evidence.

Where Is the Radical in Compound I? We believe that the most likely site of the radical in compound I is an interacting cluster or complex of functionalities comprising the side chains of Trp-191 and of a neighboring pair of methionines, Met-230 and Met-231 (see Figure 4). We are led to this proposal by the combined results of three recent experiments. First, the difference Fourier map described above fails to show any difference density near Trp-51 or Met-172 but instead does contain strong density alongside the side chain of Thr-180, which neighbors Trp-191 and Met-230. Second, a mutagenesis experiment in which Trp-51 was replaced by phenylalanine yielded a variant CCP that retained catalytic activity and exhibited the characteristic EPR radical signal associated with compound I (Fishel et al., 1987). Third, a variant CCP in which Met-172 was mutagenically replaced by serine was also active and also displayed the EPR signal (Goodin et al., 1986).

The vicinity of the proposed radical cluster is particularly noteworthy for the arrangement of oxygen atoms and aromatic groups around the two methionines. The sulfur of Met-230

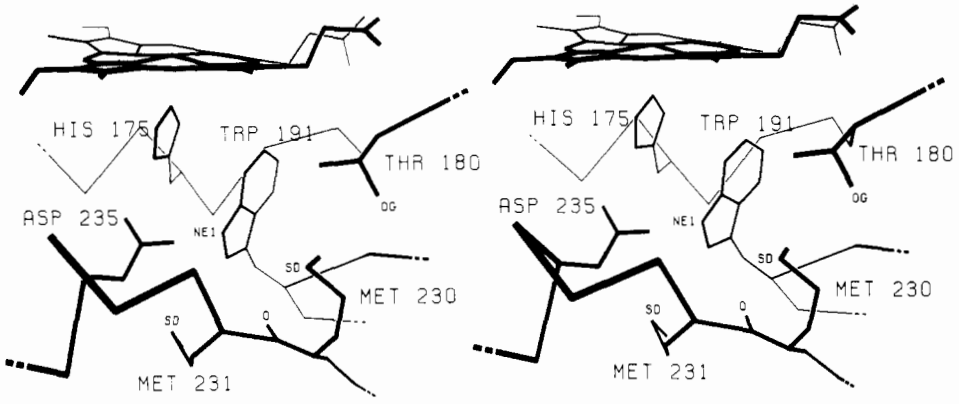

FIGURE 4: Side chains of the proposed radical cluster, Met-230, Met-231, and Trp-191. Also shown are the side chains of His-175, Thr-180, and Asp-235 as well as the heme.

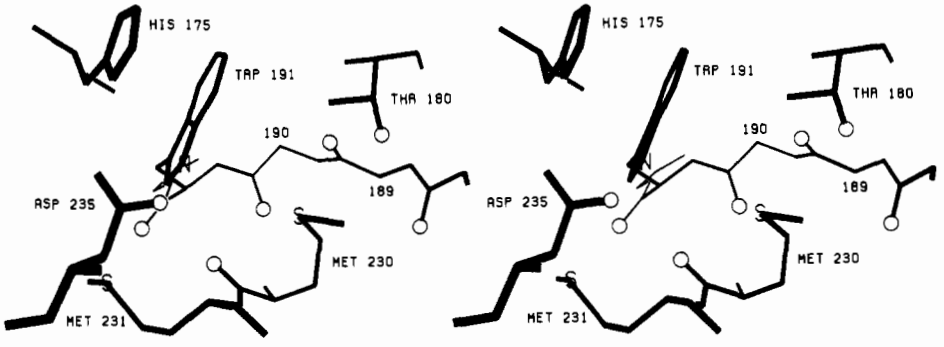

FIGURE 5: Positions of seven oxygen atoms around the sulfurs of methionines-230 and -231. The oxygens are represented by circles; five are backbone carbonyl oxygens (188, 189, 190, 191, and 230) and two belong to the side chains of Thr-180 and Asp-235. The positions of two α-carbons are indicated by the numbers 189 and 190.

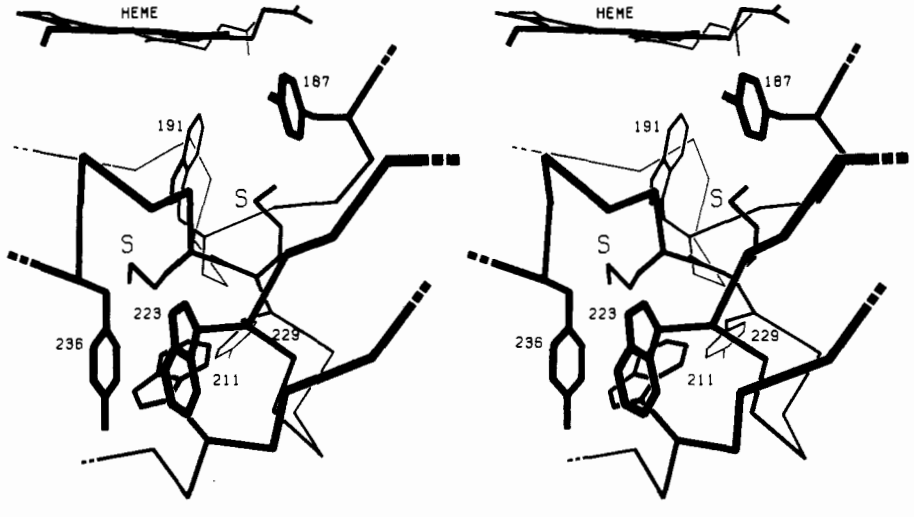

FIGURE 6: Positions of three trytophans (191, 211, and 223) and three tyrosines (187, 229, and 236) forming a pocket of aromatic rings around the two methionines, 230 and 231. Proximal histidine-175 below the heme ring is omitted for clarity.

is surrounded by four backbone carbonyl oxygens (188, 189, 190, and 230) and oxygen O^{γ} of Thr-180 (see Figure 5), all of which are 3.5–4.5 Å from the sulfur, slightly more than van der Waals contact distance. Three of these oxygens move 0.1–0.2 Å closer to the Met-230 sulfur on formation of compound I. The sulfur of Met-231 is near $O^{\gamma 2}$ of the buried carboxyl group of Asp-235 and two carbonyl oxygen atoms, 230 and 191, which are at distances of 3.8 and 5.4 Å, respectively. These carbonyl oxygens do not appear to move, but the side chain of Asp-235 moves 0.1 Å toward His-175 to maintain a hydrogen bond. Additionally, water molecule 495 moves 0.2 Å directly toward the Met-231 sulfur atom. We interpret these oxygen adjustments as signaling an increase in positive charge on the methionine sulfurs, as expected for creation of a cationic radical.

Immediately neighboring the pair of methionines are also six aromatic side chains: three tryptophans, 191, 211, and 233, and three tyrosines, 187, 229, and 236 (see Figure 6). The presence of oriented aromatic groups may help to channel charge into and out of the radical site during operation of the enzyme molecule. The position of Trp-191 is particularly curious; the indole ring of this tryptophan is parallel to and in van der Waals contact with the imidazole ring of the proximal His-175 (see Figures 3, 5, and 6). The six-membered

part of the indole ring is about 3.5 Å from the imidazole of His-175 while the five-membered part of the ring is close to both of the Met sulfurs (Trp-191 $N^{\epsilon 1}$ is about 4.5 Å from both methionine sulfurs). The position of Trp-191 suggests the existence of an electron relay system between the methionine sulfurs and the heme iron. Note also that both Trp-191 and His-175 are hydrogen bonded to the buried carboxyl group of Asp-235.

This proposed radical cluster is consistent with most of the experimental results both of Yonetani and of Hoffman and their respective co-workers. First, we point out that the lack of significant magnetic coupling between the iron and the radical site observed by EPR (Hoffman et al., 1981) and Mössbauer (Lang et al., 1976) spectroscopy suggested that they are not nearest neighbors and could be well separated. The proximity of Trp-51 or Met-172 to the iron is thus a possible argument against either as radical candidates. Although Ho et al. (1984) advanced the idea that a conformational adjustment might take place in compound I to reposition the sulfur of Met-172 further from the iron, our compound I crystal results do not show any evidence for such a movement. In contrast, the location of the 230–231 methionine pair, over 10 Å from the iron, appears more consistent with the lack of magnetic coupling. More recently, a pulsed EPR linear electric field effect measurement (Lerch et al., 1981) indicates that the radical site shares a wave function with the heme iron, which at first sight seems to imply close proximity. We address this point in the discussion of Trp-191 below.

Involvement of two methionine sulfurs as part of a radical cluster was originally suggested by Hoffman et al. (1979) on the basis of a comparison between the EPR spectrum of compound I with those of known sulfur model compounds (Musker & Wolford, 1976). Their preference for a sulfur-based radical over a tryptophan was reinforced by analysis of ENDOR measurements (Hoffman et al., 1981). However, the absence of any short sulfur–sulfur distances between neighboring methionines in the crystal structure led them to propose as an alternative a methionine sulfur radical stabilized by a nearby oxygen or nitrogen base. It now appears that the chemical requirements for the radical site suggested by Hoffman et al. may in fact be satisfied by sharing of unpaired spin density between the two methionine sulfurs of Met-230 and Met-231, stabilized by the presence of several nearby oxygen atoms.

The role of Trp-191 as part of the radical cluster may be more subtle. We suggest that the indole ring of this tryptophan is part of an electron relay linkage between the sulfur atoms and the heme iron. This idea is indirectly supported by EPR experiments of Fujita et al. (1983), who suggest that an oxidizing equivalent generated by cleavage of the peroxide bond could be transferred to a residue on the proximal side of the heme via the imidazole ring of the proximal histidine. In this context, it is suggestive that the imidazole ring of His-175 is parallel to and in van der Waals contact with the indole ring of Trp-191. In addition, our crystallographic examination of nitric oxide bound to CCP revealed that Trp-191 moves away from His-175 in this complex, indicating that this tryptophan on the proximal side of the heme can indeed be affected by a ligand on the distal side (Edwards, 1981).

Is the unpaired spin density of the radical located on Trp-191? The ENDOR experiments (Hoffman et al., 1981) argue against a tryptophan as the sole radical site. However, it must be considered possible that Trp-191 may support some minor fraction of the radical spin density. Trp-191 is hydrogen bonded to the buried Asp-235 and could therefore experience considerable charge stabilization. In addition, a pulsed EPR experiment (Lerch et al., 1981) designed to differentiate between a conventionally localized radical site and one that is somewhat delocalized (referred to by Lerch et al. as a charge-transfer center) favored the latter. The results were interpreted to mean that the radical site includes the heme iron atom. Although the methionine pair 230–231 is separated by about 10 Å from the iron, the positioning of the indole ring of Trp-191, parallel to and in van der Waals contact with the imidazole of the proximal histidine and close to the heme ring, suggests it may act as part of a bridge that would explain the effect measured in that experiment.

The compound I decay product analysis of Coulson and Yonetani (1972) also supports the picture of the radical site we propose here. Their amino acid analysis showed that tryptophans and tyrosines were the residues predominantly degraded. CCP contains a disproportionately large number of tryptophans and tyrosines as compared to, for example, horseradish peroxidase or the globins (Dayhoff, 1978), and they are most densely distributed around Met-230 and Met-231. It is therefore not surprising that these amino acids could be oxidized in the decay of compound I.

If the radical is indeed located on the proximal side of the heme, what are the implications for the mechanism of Poulos and Kraut (1980a)? First, it is probable that an electron would be transferred to create a cationic radical, rather than, as previously proposed, a hydrogen atom to create a neutral radical. Therefore, after cleavage of the peroxide bond the compound I ligand would remain as an oxygen atom bound to Fe(IV), as suggested by Simonneaux et al. (1982). To complete the catalytic cycle, compound I must then acquire two electrons from cytochrome *c* plus two hydrogen ions to reduce the ferryl oxygen atom to H_2O. We will describe possible routes for the electron and proton transfers in more detail below.

Heme–Iron Movement. As determined by least-squares refinement (described above), the iron atom in compound I is 0.2 Å from its position in the parent CCP molecule. In the parent structure the iron atom is located 0.10 Å to the proximal side of the plane of the pyrrole nitrogens while in compound I it is approximately 0.1 Å to the distal side.

At our current resolution of 2.5 Å we cannot give an exact description of the small changes in heme geometry resulting from conversion to compound I. However, we can rely on extensive analyses of hemoglobin dynamics by Perutz (1979) and by Baldwin and Chothia (1979) to guide our understanding of what to expect. First, we ask why the iron atom should reside slightly to the distal side of the heme in compound I. It might have been anticipated that the Fe(III) atom, which in the parent state is high spin ($S = {}^5/_2$) with five d electrons (Iizuka et al., 1971), would slip into the porphyrin hole on becoming low-spin ($S = 1$) Fe(IV) in compound I (Lang et al., 1976) and therefore come to rest exactly in the heme plane. However, current opinion favors the view that ligand bond distances and van der Waals interactions, rather than the oxidation state or spin state of the iron atom, dominate in determining the exact geometry of heme compounds (Warshel, 1977; Perutz, 1979; Baldwin & Chothia, 1979). The negligible influence of the iron spin state in CCP is confirmed by crystal structures of the high-spin fluoride–CCP complex (Edwards et al., 1984) and the low-spin nitric oxide–CCP complex (Edwards, 1981), both of which show the iron atom remaining slightly to the proximal side of the heme ring, as in the parent structure. Thus, the slight displacement toward the distal side observed here for CCP compound I is

probably due to an unusually short, strong Fe=O bond in the oxoferryl group. This conclusion is further supported by the results of EXAFS measurements by Chance et al. (1986a,b), which yield an Fe=O bond distance of 1.67 Å in CCP compound I, considerably shorter than either the Fe–N^{ϵ} (imidazole) bond distance of 1.91 Å or the Fe–O distances of 1.83 Å in oxymyoglobin and 1.88 Å in aquomyoglobin. Similar heme geometry is seen in the crystal structure of the oxyhemoglobin β-subunit in which the iron atom is displaced 0.10 Å toward the distal side (Shaanan, 1983).

Electron Transfer and the Complex with Cytochrome c. A hypothetical model for the CCP–cytochrome *c* complex, based on model-building experiments, was proposed by Poulos and Kraut (1980b). The main principle guiding the construction of the model was matching of conserved lysine residues on the surface of cytochrome *c* with negatively charged residues around the heme crevice of CCP. An excellent stereochemical fit between the two molecules was obtained, and in addition, the model was consistent with information from cross-linking experiments (Bisson & Capaldi, 1981) and measurements of the heme–heme separation (Gupta & Yonetani, 1973; Leonard & Yonetani, 1974). The original model required minor adjustments (Poulos & Finzel, 1984) after least-squares refinement of the CCP structure (Finzel et al., 1984). Most notably, the refinement required correction of positions of residues 180–183, indicating that His-181 is hydrogen bonded directly to the propionate of heme pyrrole IV.

Since the hypothetical model was first proposed, the complex has been examined by chemical modification experiments, which support its validity. Specifically, photooxidation experiments (Bosshard et al., 1984) confirm the model-based prediction of His-181 as a residue at the intermolecular interface. In addition, an analysis of CCP cross-linked to cytochrome *c* by chemical modification of carboxyl groups (Waldmeyer et al., 1982) supports the assignment of complementary charge-paired residues in the model.

Least-squares refinement of compound I, described above, reveals a coordinated movement of the loop 175–190. Our interest is attracted to movements of this loop because it forms part of the proposed binding surface for cytochrome *c*. Although the magnitude of the twisting motion is small, it is worth describing two details that may be significant for the interaction between compound I and cytochrome *c*: the movements of His-181 and Lys-183.

The position of the His-181 imidazole ring remains fixed while its backbone chain atoms tend to follow the heme's movement of about 0.1 Å further into the heme crevice. The imidazole ring thus remains parallel to the hemes of both proteins, a feature considered important for electron transfer via adjacent π orbitals (Poulos & Kraut, 1980b). This parallel orientation of rings maintained in compound I leads us to hypothesize that the electron from cytochrome *c* may pass through the imidazole ring of His-181 directly into the CCP heme group. The importance of the heme propionates to the possible function of His-181 is underscored by the experiment of Asakura and Yonetani (1969), which showed that esterification of the propionates reduces the rate of electron transfer by a factor of about 200 without interfering with either formation of compound I or binding of cytochrome *c*.

Also worthy of note is the side chain of Lys-183, which is missing in the room temperature parent structure due to disorder, but is ordered in the lower temperature structure as far as C^{δ} extending straight out from the molecule into the solvent. In contrast to His-181, the C^{α} of Lys-183 remains stationary, but its side chain rotates to cause the C^{δ} to move by 0.3 Å. In the absence of an experimentally determined structure for the CCP–cytochrome *c* complex, we cannot yet tell what the function of this movement might be. However, in our model of the complex, Lys-183 is the residue that most closely approaches the heme of cytochrome *c*. Takano and Dickerson (1980, 1981) have argued that a movement of the cytochrome *c* heme into its hydrophobic crevice by 0.15 Å serves to stabilize the reduced oxidation state. The approach by Lys-183 of CCP may increase the polarity near the crevice, perhaps to promote the electron-transfer event.

Proton Transfer and Role of Arg-48. An important residue near the peroxide binding site is Arg-48. We have previously proposed that its guanidinium group participates in the O–O bond cleavage by promoting negative charge buildup on the oxygen of the leaving group, ROH (Poulos & Kraut, 1980a). The Arg-48 side chain is flexible, as demonstrated by the CCP complex with HF (Edwards et al., 1984) in which it repositions to optimize its interaction with the bound fluoride.

In compound I, Arg-48 moves toward the ligand site indicating a strong hydrogen bond to the ferryl oxygen atom. In addition, the guanidinium group of Arg-48 also maintains hydrogen bonds on its opposite side to water molecules leading to the solvent. Since two protons (in addition to two electrons) are required to convert the oxygen ligand into H_2O, it is possible that these protons are conveyed from the solvent to the ligand site via Arg-48. Another possible path for protons is through a chain of water molecules occupying a channel leading from the solvent into the distal-side heme cavity, which in fact may also function as the ligand access channel (Poulos et al., 1980; Finzel et al., 1984).

ACKNOWLEDGMENTS

We thank Dr. Matthew Mauro for suggesting many important ideas used in this paper, Dr. Thomas Poulos for help in initially planning the experiment, and Laurence Fishel and also Michael Smith and David Goodin for making their mutagenesis results available to us prior to publication. We are grateful to Chris Nielsen for helping with the data collection and for modifying the software to make this experiment possible. We credit the expertise of Donald Sullivan in building and maintaining the Mark II low-temperature device used in X-ray data collection and of Stephen Dempsey in developing the molecular modeling system program for computer graphics.

Registry No. CCP, 9029-53-2; Fe, 7439-89-6; heme, 14875-96-8.

REFERENCES

Abrams, R., Altschul, A. M., & Hogness, T. R. (1942) *J. Biol. Chem. 142*, 303–316.

Asakura, T., & Yonetani, T. (1969) *J. Biol. Chem. 244*, 4573–4579.

Baldwin, J., & Chothia, C. (1979) *J. Mol. Biol. 129*, 175–220.

Bisson, R., & Capaldi, R. A. (1981) *J. Biol. Chem. 256*, 4362–4367.

Bosshard, H. R., Banziger, J., Hasler, T., & Poulos, T. L. (1984) *J. Biol. Chem. 259*, 5683–5690.

Chance, B., Powers, L., Ching, Y., Poulos, T., Schonbaum, G. R., Yamazaki, I., & Paul, K. G. (1984) *Arch. Biochem. Biophys. 235*, 596–611.

Chance, M., Powers, L., Kumar, C., & Chance, B. (1986a) *Biochemistry 25*, 1259–1265.

Chance, M., Powers, L., Poulos, T., & Chance, B. (1986b) *Biochemistry 25*, 1266–1270.

Coulson, A. F., & Yonetani, T. (1972) *Biochem. Biophys. Res. Commun. 49*, 391–398.

Dayhoff, M. O., Ed. (1978) *Atlas of Protein Sequence and Structure*, Vol. 5, Supplement 3, National Biomedical

Research Foundation, Silver Springs, MD.
Dolphin, D., Forman, A., Borg, D. C., Fajer, J., & Felton, R. H. (1971) *Proc. Nat. Acad. Sci. U.S.A. 68*, 614–618.
Edwards, S. L. (1981) Ph.D. Dissertation, University of California, San Diego.
Edwards, S. L., Poulos, T. L., & Kraut, J. (1984) *J. Biol. Chem. 259*, 12984–12988.
Erecinska, M., Oshino, N., Loh, P., & Brocklehurst, E. (1973) *Biochim. Biophys. Acta 292*, 1–12.
Erman, J. E., & Yonetani, T. (1975) *Biochim. Biophys. Acta 393*, 350–357.
Finzel, B. C., Poulos, T. L., & Kraut, J. (1984) *J. Biol. Chem. 259*, 13027–13036.
Fishel, L. A., Villafranca, J. E., Mauro, J. M., & Kraut, J. (1987) *Biochemistry 26*, 351–360.
Fujita, I., Hanson, L. K., Walker, F. A., & Fajer, J. (1983) *J. Am. Chem. Soc. 105*, 3296–3300.
Goodin, D. B., Mauk, A. G., & Smith, M. (1986) *Proc. Natl. Acad. Sci. U.S.A. 83*, 1295–1299.
Gupta, R. K., & Yonetani, T. (1973) *Biochim. Biophys. Acta 292*, 502–508.
Hall, S. R., Stewart, J. M., & Munn, R. J. (1980) *Acta Crystallogr. Sect. A: Cryst. Phys., Diffr., Theor. Gen. Crystallogr. A36*, 979–989.
Hendrickson, W. A., & Konnert, J. H. (1980) in *Computing in Crystallography* (Diamond, R., Ramaseshan, S., & Venkatesan, K., Eds.) pp 13.1–13.23, Indian Institute of Science, Bangalore, India.
Ho, P. S., Hoffman, B. M., Soloman, N., Kang, C. H., & Margoliash, E. (1984) *Biochemistry 23*, 4122–4128.
Hoffman, B. M., Roberts, J. E., Brown, T. G., Kang, C. H., & Margoliash, E. (1979) *Proc. Natl. Acad. Sci. U.S.A. 76*, 6132–6136.
Hoffman, B. M., Roberts, J. E., Kang, C. H., & Margoliash, E. (1981) *J. Biol. Chem. 256*, 6556–6564.
Howard, A. J., Nielsen, C., & Xuong, Ng. h. (1985) *Methods Enzymol. 114*, 452–472.
Iizuka, T., Kotani, M., & Yonetani, T. (1971) *J. Biol. Chem. 246*, 4731–4736.
Lang, G., Spartalian, K., & Yonetani, T. (1976) *Biochim. Biophys. Acta 451*, 250–258.
Leonard, J. J., & Yonetani, T. (1974) *Biochemistry 13*, 1465–1468.
Lerch, K., Mims, W. B., & Peisach, J. (1981) *J. Biol. Chem. 256*, 10088–10091.
Musker, W. K., & Wolford, T. L. (1976) *J. Am. Chem. Soc. 98*, 3055–3056.
Nelson, C. E., Sitzman, E. V., Kang, C. H., & Margoliash, E. (1977) *Anal. Biochem. 83*, 622–631.
Perutz, M. F. (1979) *Annu. Rev. Biochem. 48*, 327–386.
Poulos, T. L., & Kraut, J. (1980a) *J. Biol. Chem. 255*, 8199–8205.
Poulos, T. L., & Kraut, J. (1980b) *J. Biol. Chem. 255*, 10322–10330.
Poulos, T. L., & Finzel, B. C. (1984) *Pept. Protein Rev. 4*, 115–171.
Poulos, T. L., Freer, S. T., Alden, R. A., Xuong, Ng. h., Edwards, S. L., Hamlin, R. C., & Kraut, J. (1978) *J. Biol. Chem. 253*, 3730–3735.
Poulos, T. L., Freer, S. T., Alden, R. A., Edwards, S. L., Skogland, U., Takio, T., Eriksson, B., Xuong, Ng. h., Yonetani, T., & Kraut, J. (1980) *J. Biol. Chem. 255*, 575–580.
Shaanan, B. (1983) *J. Mol. Biol. 171*, 31–59.
Simonneaux, G., Scholz, W. F., Reed, C. A., & Lang, G. (1982) *Biochim. Biophys. Acta 716*, 1–7.
Takano, T., & Dickerson, R. E. (1980) *Proc. Natl. Acad. Sci. U.S.A. 77*, 6371–6375.
Takano, T., & Dickerson, R. E. (1981) *J. Mol. Biol. 153*, 95–115.
Thaller, C., Weaver, L. H., Eichele, G., Wilson, E., Karlsson, R., & Jansonius, J. N. (1981) *J. Mol. Biol. 147*, 465–469.
Waldmeyer, B., Bechtold, R., Bosshard, H. R., & Poulos, T. L. (1982) *J. Biol. Chem. 257*, 6073–6076.
Warshel, A. (1977) *Proc. Natl. Acad. Sci. U.S.A. 74*, 1789–1793.
Xuong, Ng. h., Freer, S. T., Hamlin, R., Nielsen, C., & Vernon, W. (1978) *Acta Crystallogr., Sect. A: Cryst. Phys., Diffr., Theor. Gen. Crystallogr. A34*, 289–296.
Yonetani, T., & Ray, G. S. (1965) *J. Biol. Chem. 240*, 4503–4508.
Yonetani, T., & Ray, G. S. (1966) *J. Biol. Chem. 241*, 700–706.
Yonetani, T., Chance, B., & Kajiwara, S. (1966a) *J. Biol. Chem. 241*, 2981–2982.
Yonetani, T., Schleyer, H., & Ehrenberg, A. (1966b) *J. Biol. Chem. 241*, 3240–3243.